Available online at www.sciencedirect.com

ScienceDirect

Mendeleev Commun., 2024, **34**, 711–714

Mendeleev Communications

The impact of the porous structure on the efficiency of PdIn methanol synthesis catalysts

Alexander V. Rassolov,*[a] Galina N. Baeva,[a] Dmitry P. Melnikov,[a,b] Artem R. Kolyadenkov,[a] Anastasia E. Vaulina[a] and Alexander Yu. Stakheev[a]

[a] *N. D. Zelinsky Institute of Organic Chemistry, Russian Academy of Sciences, 119991 Moscow, Russian Federation. E-mail: rav@ioc.ac.ru*

[b] *National University of Oil and Gas 'Gubkin University', 119991 Moscow, Russian Federation*

DOI: 10.1016/j.mencom.2024.09.028

The characteristics of the porous structure and the specific surface area of the support have a significant impact on both the structure of the active sites and the efficiency of catalysts for the synthesis of methanol from CO_2. The use of a complex of physicochemical methods of analysis in combination with the results of catalytic experiments has enabled the main tendencies in the development of productive and selective catalysts based on PdIn intermetallic nanoparticles to be established.

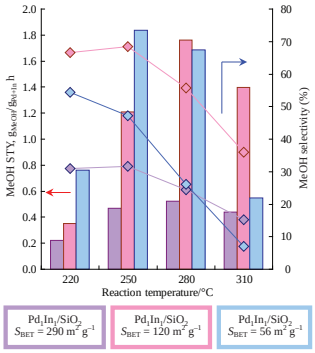

Keywords: Pd–In intermetallics, nanoparticles formation, methanol synthesis, CO_2 hydrogenation, metal–support interactions.

The potential of intermetallic compositions to act as effective catalysts for the methanol synthesis from carbon dioxide has been a subject of active investigation in recent decades. This is an important research area in both heterogeneous catalysis and green chemistry.[1–5] It contributes to the solution of the problem of carbon dioxide emissions into the atmosphere and its effective utilization. Furthermore, a wide selection of intermetallics[6,7] and their unique features [8–10] afford the opportunity to control and fine-tune their structural and catalytic characteristics by varying the composition and ratio of components at the preparation stage.[1,11–13] It has a direct impact on both the phase composition of resulting nanoparticles and the structure of active sites, at which the target reaction directly occurs.

It is also crucial to select the optimal support that possesses the necessary characteristics to achieve maximum activity and target product selectivity. The primary parameters of the support that influence the formation of the intermetallic compound highly ordered structure are its acid–base properties,[14] stability under high-temperature treatment,[15,16] porous structure and specific surface area.[17] The latter has a significant impact on the homogeneity of the resulting intermetallic nanoparticles and largely determines the process direction. The specific surface area is a crucial factor in regulating the dispersion and distribution of the active component throughout the nanoparticle.

The exceptional importance of this support characteristic is confirmed by numerous reports on the study of the impact of support specific surface area on the catalytic performance. The subject of these publications is mainly $Cu/ZnO/Al_2O_3$, a traditional catalyst for methanol synthesis.[18–22] It should be noted, however, that such studies using supported intermetallic catalysts have not yet previously been presented in practice.

The main goal of this study was to identify the correlation between the features of the porous structure, the specific surface area of the support and the catalytic characteristics of intermetallic PdIn catalysts for the carbon dioxide hydrogenation to methanol. In order to perform a correct comparative study and to establish correlations between catalytic characteristics and porous structure, SiO_2 was used as a support in this work. The specific surface area of the support varied from 56 to 120 and 290 $m^2\ g^{-1}$. The choice of SiO_2 is based on promising results obtained in one of our previous studies.[12]

The choice of PdIn intermetallic compositions was dictated by several factors. These include the ease of use of PdIn compositions as model catalytic systems, as well as impressive results on carbon dioxide conversion. Analysis of literature shows that PdIn intermetallic compounds represent a promising alternative to traditional $Cu/ZnO/Al_2O_3$ catalysts for methanol synthesis. Their efficiency is in many cases comparable to that of the above-mentioned catalysts, and in some cases even superior.[1,2,23] This is largely due to the more efficient activation of the CO_2 molecule compared to the $Cu/ZnO/Al_2O_3$ catalyst, which is ensured by the unique structure of heteroatomic active sites consisting of single Pd and an adjacent In atom. This structure facilitates the reduction of the activation energy of the CO_2 molecule and ensures its step-by-step hydrogenation, initially to a formate intermediate and subsequently to the target reaction product, namely a methanol molecule.[12] PdIn intermetallic nanoparticles were synthesized using the traditional method of incipient wetness impregnation of the support.

Figure 1 illustrates the typical diffraction patterns of monometallic Pd and In reference samples, as well as synthesized PdIn catalysts in the angle range 2θ = 32–60°. It is

widely acknowledged that one of the primary challenges in studying the phase composition of supported intermetallic nanoparticles is the overlapping of the phase signals between the resulting intermetallic compound and the support due to the low crystallinity of the latter.[23] In the specified angle range for all PdIn samples, the presence of characteristic reflections was noted in the intervals 2θ = 37.5–42.4° and 55.7–57.9°. The positions of these signals are in good agreement with the data in the crystallographic database and may correspond to the positions of the main signals of the cubic structure of the CsCl type of Pd_1In_1 intermetallic phase (PDF 04-004-1991). However, the significant width of the main signal in the diffraction pattern of $PdIn/SiO_2$ (290) sample may indicate the presence of a certain amount of PdIn phase depleted in Pd. It should be noted that no reflections indicative of the potential presence of other intermetallic compounds or monometallic Pd phases were observed in the diffraction patterns of other catalysts. This is attributed to the high stability of this intermetallic compound over a wide range of Pd concentrations.[24,25] The Rietveld method was employed to conduct quantitative calculations of the phase composition. The results indicated that the intermetallic phase content was approximately 3% for all studied samples. However, a more detailed analysis of the $PdIn/SiO_2$ (290) and $PdIn/SiO_2$(56) patterns revealed the presence of a low-intensity reflection with a maximum at 2θ = 32.9°, which can be attributed to the main signal of the tetragonal phase (101) of metallic In (JCPDS 85–1409). It is also noteworthy that the average nanoparticles size calculation, performed using the Scherrer equation, indicated that the nanoparticle size exhibited a slight dependence on the specific area of the support, with a relatively narrow range of variation from 6.1 to 4.4 nm (see Table S1).

The obtained results indicate that the composition of the formed intermetallic PdIn nanoparticles is in close correspondence to the composition specified during the preparation stage. Concurrently, the diffraction pattern of the $PdIn/SiO_2$ (120) sample does not exhibit reflections of monometallic Pd and In components, which may suggest the high homogeneity of the nanoparticles.

The results of the investigation of the catalysts surface structure using IR spectroscopy of adsorbed CO are presented in Figure 2.

The analysis of Pd monometallic reference sample spectra revealed the presence of several CO adsorption bands. The presence of a low-intensity adsorption band in the range from 2110 to 2030 cm^{-1} indicates the presence of CO adsorption sites comprising one Pd atom (linear adsorption sites). Conversely, the presence of broad signals in the range of 2000–1875 cm^{-1} is

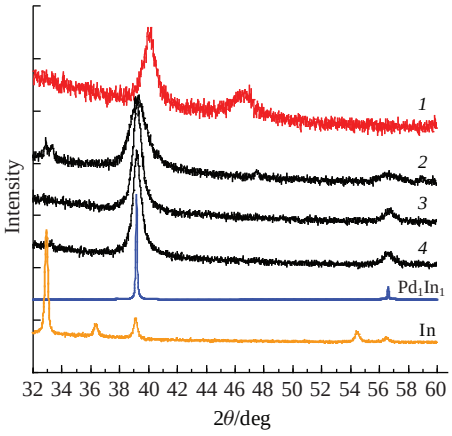

Figure 1 XRD patterns for the samples of (*1*) Pd/SiO_2 (120), (*2*) $PdIn/SiO_2$ (290), (*3*) $PdIn/SiO_2$ (120), (*4*) $PdIn/SiO_2$ (56).

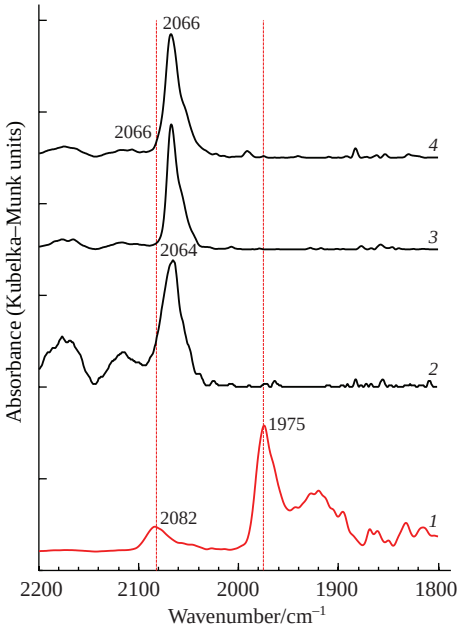

Figure 2 DRIFT spectra of adsorbed CO on the samples of (*1*) Pd/SiO_2 (120), (*2*) $PdIn/SiO_2$ (290), (*3*) $PdIn/SiO_2$ (120), (*4*) $PdIn/SiO_2$ (56).

indicative of active sites comprising two or three neighboring Pd atoms (multiatomic adsorption sites).[26]

The spectra of the intermetallic PdIn samples revealed only signals related to linear CO adsorption. It is important to note that regardless of the support, the position of the signal maxima is shifted towards lower wave numbers relative to the monometallic sample, with values ranging from 2064 to 2066 cm^{-1}. The observed shift indicates a decrease in dipole interactions in neighboring CO molecules due to the isolation of Pd_1 adsorption sites by In atoms, as well as a weakening of the C–O bond. This process occurs as the result of a redistribution of electron density between Pd atoms and carbon monoxide molecules that have been adsorbed on them.[23,27] The results are in agreement with data obtained in a number of other studies, which report a low probability of multiatomic adsorption of CO on the surface of PdIn intermetallic compounds due to the absence of Pd_n adsorption sites ($n \geqslant 2$) and the preferential formation of isolated Pd_1 sites.[7,28,29] These sites are constituted by single palladium atoms, which are separated from each other by atoms of a second metal, specifically indium atoms. In this instance, the isolation of the Pd atoms results in a significant increase in the distance between them, which makes the adsorption of CO on two atoms impossible.[30]

The results of the low-temperature nitrogen adsorption experiments on the synthesized samples are presented in Figures 3(*a*),(*b*) and Table S1.

The shape of the adsorption–desorption isotherms corresponds to type IV according to the IUPAC classification, which is indicative of mesoporous materials. In this case, for the $PdIn/SiO_2$ (56) and $PdIn/SiO_2$ (120) samples, the shape of the hysteresis loop allows us to conclude that there are cylindrical pores. However, in case of $PdIn/SiO_2$ (290) catalyst, the hysteresis loop has a shape more characteristic of materials with a disordered porous structure. In such materials, the shape is not strictly defined. These materials are characterized by the presence of a large number of pores, with an average size of less than 4 nm. This conclusion is confirmed by the data in Figure 3(*b*). It is important to note that the average pore sizes in the $PdIn/SiO_2$ (120) and $PdIn/SiO_2$ (56) samples (38.1 and 12.6 nm, respectively) are significantly larger than that of $PdIn/SiO_2$ (290) sample (4.9 nm). A notable disparity in pore dimensions can

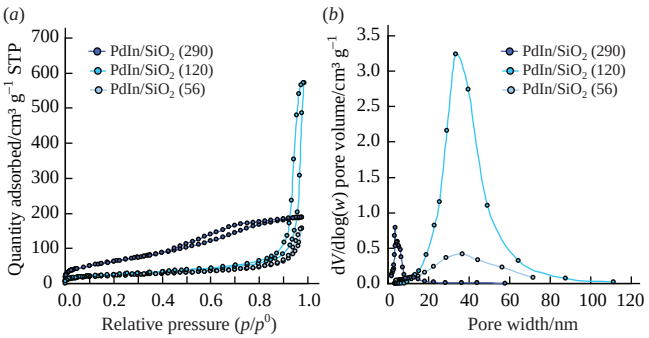

Figure 3 (*a*) Adsorption–desorption isotherms and (*b*) pore size distribution curves for intermetallic PdIn catalysts.

facilitate accelerated diffusion of reaction byproduct molecules, namely water. This process serves to prevent the oxidation of one of the catalyst's active components (Pd), and also to prevent subsequent deactivation.[21,31] Additionally, it was determined that the pore volume in the PdIn/SiO_2 (120) sample is 0.89 $cm^3\ g^{-1}$, while for PdIn/SiO_2 (56) and PdIn/SiO_2 (290) this value is much lower (0.24 and 0.27 $cm^3\ g^{-1}$, respectively). As previously documented in the literature, metal oxides with a developed porous structure can enhance catalytic performance by limiting the growth of active sites and improving the mass transfer of reagent molecules in the pores.[17]

The catalytic characteristics of the synthesized PdIn samples were investigated in gas-phase hydrogenation of carbon dioxide into methanol reaction.

The obtained results are presented in Figures 4(*a*),(*b*). A study of the influence of temperature on the conversion of carbon dioxide revealed that the individual supports SiO_2 (290) and SiO_2 (56) did not exhibit any catalytic activity under the specified process conditions. While, SiO_2 (120) and In/SiO_2 (120) exhibit

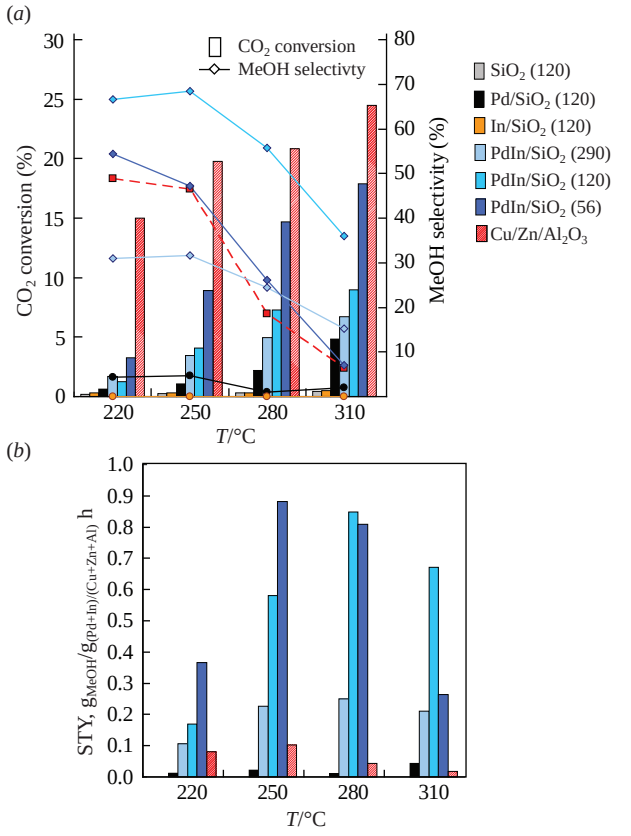

Figure 4 (*a*) CO_2 conversion rate, methanol selectivity and (*b*) methanol STY dependences on the reaction temperature. The process conditions: 220–310 °C, 3.5 MPa, GHSV = 3000 h^{-1}, $CO_2:H_2 = 1:3$.

minimal activity. Consequently, the maximum conversion achieved for these samples at 310 °C was 0.44 and 0.53%, respectively. The only carbon-containing product identified for these samples was carbon monoxide. The formation of this compound is associated with the occurrence of a competitive transformation of the reverse water gas-shift reaction, which intensifies with increasing process temperature.[32] A slightly higher conversion (4.8%) was obtained with the monometallic sample Pd/SiO_2 (120), however its methanol selectivity over the entire temperature range does not exceed 4.5%.

The results obtained for a series of PdIn samples deposited on SiO_2 were analyzed. The findings indicated that a reduction in S_{BET} led to an activity increase. Thus, at 250 °C, CO_2 conversion for the PdIn/SiO_2 (290) and PdIn/SiO_2 (56) samples is 3.5 and 8.9%, respectively. It is noteworthy that the methanol selectivity reaches maximum (S_{MeOH} = 68.4%) at this temperature on the PdIn/SiO_2 (120) sample. This value is markedly superior to the characteristics of not only all intermetallic samples, but also of the Cu/ZnO/Al_2O_3 reference catalyst, the maximum selectivity of which is 48.9% at a low temperature of 220 °C. The observed high efficiency of PdIn/SiO_2 (56) and PdIn/SiO_2 (120) may be attributed to the combined influence of various factors. These may include the high homogeneity of the resulting nanoparticles, which is confirmed by the results of X-ray phase analysis and IR spectroscopy of adsorbed CO presented above. The structure of heteroatomic PdIn active sites, which were previously discussed, consists of a single Pd atom and an adjacent In atom also has a significant direct impact on the selectivity of intermetallic catalysts.[12] It is clear that support parameters, such as the average pore size and their volume, can also have a significant impact on the process efficiency. This assumption is also validated by the data obtained through the low-temperature nitrogen adsorption method presented above. It is important to highlight the positive impact of all these factors on the catalysts performance. It was found the highest productivity was achieved when the PdIn/SiO_2 (56) and PdIn/SiO_2 (120) catalysts were used. The maximum methanol productivity was 0.88 and 0.85 $g_{MeOH}/g_{(Pd+In)}$ h, respectively, which represents a productivity enhancement of more than 8 times compared to that of traditional methanol synthesis catalyst [0.10 $g_{MeOH}/g_{(Cu+Zn+Al)}$ h].

Thus, we can conclude that the efficiency of intermetallic catalysts for the synthesis of methanol from CO_2 largely depends on the structural features of the support used. This work presents the results of a comprehensive physicochemical study of PdIn catalysts deposited on the surface of SiO_2 with different specific surface areas. The study identified key factors influencing the target process. As shown by IR spectroscopy of adsorbed CO and X-ray phase analysis, the use of SiO_2 as a support, S_{BET} = 56 and 120 $m^2\ g^{-1}$, promotes the formation of more homogeneous intermetallic nanoparticles of a given composition, the average size of which varies from 6.1 to 5.8 nm, respectively. This has a positive effect on the catalytic characteristics of these samples, in which the highest productivity [0.88 $g_{MeOH}/g_{(Pd+In)}$ h] and methanol selectivity (68.4%) were obtained. As the main reasons for the high homogeneity of PdIn nanoparticles, it is necessary to highlight the features of the porous structure of the supports used. These include the pore volume, which in case of PdIn/SiO_2 (120) sample is 0.89 $cm^3\ g^{-1}$, a value that is significantly higher than that of other catalysts. Another factor that has an impact on the uniformity of nanoparticles is the average pore size. For the PdIn/SiO_2 (56) and PdIn/SiO_2 (120) samples, this value is 12.6 and 38.1 nm, respectively. For the PdIn/SiO_2 (290) catalyst, it does not exceed 4.8 nm. It can be concluded that an increase in the specific surface area does not contribute to an increase in both selectivity and methanol productivity.

This work was supported by the Russian Science Foundation (grant no. 23-23-00510).

Online Supplementary Materials

Supplementary data associated with this article can be found in the online version at doi: 10.1016/j.mencom.2024.09.028.

References

1 J. L. Snider, V. Streibel, M. A. Hubert, T. S. Choksi, E. Valle, D. C. Upham, J. Schumann, M. S. Duyar, A. Gallo, F. Abild-Pedersen and T. F. Jaramillo, *ACS Catal.*, 2019, **9**, 3399.
2 A. García-Trenco, A. Regoutz, E. R. White, D. J. Payne, M. S. P. Shaffer and C. K. Williams, *Appl. Catal., B*, 2018, **220**, 9.
3 N. Rui, Z. Wang, K. Sun, J. Ye, Q. Ge and C.-j. Liu, *Appl. Catal., B*, 2017, **218**, 488.
4 Y. Wang, D. Wu, T. Liu, G. Liu and X. Hong, *J. Colloid Interface Sci.*, 2021, **597**, 260.
5 P. Sharma, P. Hoang Ho, J. Shao, D. Creaser and L. Olsson, *Fuel*, 2023, **331**, 125878.
6 S. Furukawa and T. Komatsu, *ACS Catal.*, 2017, **7**, 735.
7 S. Furukawa, M. Endo and T. Komatsu, *ACS Catal.*, 2014, **4**, 3533.
8 V. S. Marakatti and S. C. Peter, *Prog. Solid State Chem.*, 2018, **52**, 1.
9 A. Dasgupta and R. M. Rioux, *Catal. Today*, 2019, **330**, 2.
10 S. E. Collins, J. J. Delgado, C. Mira, J. J. Calvino, S. Bernal, D. L. Chiavassa, M. A. Baltanás and A. L. Bonivardi, *J. Catal.*, 2012, **292**, 90.
11 O. A. Ojelade, S. F. Zaman, M. A. Daous, A. A. Al-Zahrani, A. S. Malik, H. Driss, G. Shterk and J. Gascon, *Appl. Catal., A*, 2019, **584**, 117185.
12 A. V. Rassolov, G. N. Baeva, A. R. Kolyadenkov, P. V. Markov and A. Yu. Stakheev, *Russ. Chem. Bull.*, 2023, **72**, 2583.
13 R. Manrique, J. Rodríguez-Pereira, S. A. Rincón-Ortiz, J. J. Bravo-Suárez, V. G. Baldovino-Medrano, R. Jiménez and A. Karelovic, *Catal. Sci. Technol.*, 2020, **10**, 6644.
14 O. Oyola-Rivera, M. A. Baltanás and N. Cardona-Martínez, *J. CO_2 Util.*, 2015, **9**, 8.
15 A. Ota, E. L. Kunkes, I. Kasatkin, E. Groppo, D. Ferri, B. Poceiro, R. M. Navarro Yerga and M. Behrens, *J. Catal.*, 2012, **293**, 27.
16 Q. Wu, S. Liang, T. Zhang, B. Louis and Q. Wang, *Fuel*, 2022, **313**, 122963.
17 X. Jiang, X. Nie, X. Guo, C. Song and J. G. Chen, *Chem. Rev.*, 2020, **120**, 7984.
18 Y. Zhang, Q. Sun, J. Deng, D. Wu and S. Chen, *Appl. Catal., A*, 1997, **158**, 105.
19 G. Bonura, M. Cordaro, C. Cannilla, F. Arena and F. Frusteri, *Appl. Catal., B*, 2014, **152**–**153**, 152.
20 W. Cai, P. R. de la Piscina, J. Toyir and N. Homs, *Catal. Today*, 2015, **242**, 193.
21 T. Witoon, J. Chalorngtham, P. Dumrongbunditkul, M. Chareonpanich and J. Limtrakul, *Chem. Eng. J.*, 2016, **293**, 327.
22 X. Dong, F. Li, N. Zhao, F. Xiao, J. Wang and Y. Tan, *Appl. Catal., B*, 2016, **191**, 8.
23 A. V. Rassolov, P. V. Markov, G. N. Baeva, D. A. Bokarev, A. R. Kolyadenkov, A. E. Vaulina and A. Yu. Stakheev, *Mendeleev Commun.*, 2023, **33**, 673.
24 M. Neumann, D. Teschner, A. Knop-Gericke, W. Reschetilowski and M. Armbrüster, *J. Catal.*, 2016, **340**, 49.
25 H. Okamoto, *J. Phase Equilib.*, 2003, **24**, 481.
26 G. Agostini, R. Pellegrini, G. Leofanti, L. Bertinetti, S. Bertarione, E. Groppo, A. Zecchina and C. Lamberti, *J. Phys. Chem. C*, 2009, **113**, 10485.
27 K. Föttinger, J. A. van Bokhoven, M. Nachtegaal and G. Rupprechter, *J. Phys. Chem. Lett.*, 2011, **2**, 428.
28 T. Hirano, Y. Kazahaya, A. Nakamura, T. Miyao and S. Naito, *Catal. Lett.*, 2007, **117**, 73.
29 I. S. Mashkovsky, P. V. Markov, G. O. Bragina, G. N. Baeva, A. V. Rassolov, I. A. Yakushev, M. N. Vargaftik and A. Yu. Stakheev, *Nanomaterials*, 2018, **8**, 769.
30 N. S. Smirnova, G. N. Baeva, P. V. Markov, I. S. Mashkovsky, A. V. Bukhtiyarov, Y. V. Zubavichus and A. Yu. Stakheev, *Mendeleev Commun.*, 2022, **32**, 807.
31 S. Kattel, P. J. Ramirez, J. G. Chen, J. A. Rodriguez and P. Liu, *Science*, 2017, **355**, 1296.
32 J. Nakamura, *Top. Catal.*, 2003, **22**, 277.

Received: 6th June 2024; Com. 24/7529